

Diminished efficiency in the oceanic silica pump caused by bacteria-mediated silica dissolution

*Kay D. Bidle*¹

Marine Biology Research Division, Scripps Institution of Oceanography, University of California San Diego, 9500 Gilman Drive, La Jolla, California 92093-0202

Mark A. Brzezinski

Department of Ecology, Evolution, and Marine Biology and the Marine Science Institute, University of California, Santa Barbara, California 93106

*Richard A. Long*²

Marine Biology Research Division, Scripps Institution of Oceanography, University of California San Diego, 9500 Gilman Drive, La Jolla, California 92093-0202

Janice L. Jones

Department of Ecology, Evolution, and Marine Biology and the Marine Science Institute, University of California, Santa Barbara, California 93106

Farooq Azam

Marine Biology Research Division, Scripps Institution of Oceanography, University of California San Diego, 9500 Gilman Drive, La Jolla, California 92093-0202

Abstract

Previous laboratory findings indicated that marine bacteria accelerate biogenic silica (bSiO₂) dissolution rates in the sea by degrading the organic coating surrounding diatom frustules and exposing the underlying silica to chemical attack by undersaturated seawater. We examined the effectiveness of bacterial activity in facilitating in situ bSiO₂ dissolution during a diatom bloom in Monterey Bay, California, following moderate upwelling. Inhibition of bacterial activity with antibiotics and protease inhibitors reduced specific bSiO₂ dissolution rates (V_{dis}) at five of six stations, with a reduction of $44 \pm 27\%$ (mean \pm SD, $n = 6$, range 22–91%) over 24 h. Reduced V_{dis} in inhibitor treatments corresponded with reductions in abundance, production, and proteolytic activity of attached bacteria. Dissolution rates were highly correlated with protease activity integrated from the surface down to the depth where each dissolution was measured, suggesting that increased V_{dis} with depth in the upper 20–80 m of the ocean is caused by the progressive removal of organic matter from frustules during sinking. Facilitation of bSiO₂ dissolution by in situ bacterial assemblages varied between stations and was likely influenced by the physiological condition of resident diatom assemblages. Denaturing gradient gel electrophoresis and 16S rRNA gene sequencing of bacteria colonizing in situ diatom assemblages confirmed previous findings that specific bacterial phylotypes (Cytophaga/Flavobacteria/Bacteriodes; α and γ subclasses of *Proteobacteria*) mediate bSiO₂ dissolution.

The importance of diatoms to marine primary productivity has led to an examination of factors that control their growth (Thompson 1999; Martin-Jézéquel et al. 2000). Silicic acid supply mechanisms have been emphasized because diatoms have an absolute silicon requirement for growth

¹ To whom correspondence should be addressed. Present address: Institute of Marine and Coastal Science, Rutgers University, 71 Dudley Road, New Brunswick, New Jersey 08901.

² Present address: Department of Oceanography, Texas A&M University, College Station, Texas 77843-3146.

Acknowledgments

We thank the captain and crew of the R/V *Point Sur* for their help and cooperation at sea. This research was supported by NSF grants OCE-9819603 to F.A. and OCE-9904410 to M.A.B. The comments of two anonymous reviewers helped to strengthen this manuscript.

(Lewin 1962) and experience limitation of silicic acid uptake in a variety of ocean environments (Nelson and Brzezinski 1990; Nelson and Tréguer 1992; Brzezinski and Nelson 1996; Nelson and Dortch 1996; Brzezinski et al. 1998). The concept of the “silica pump” (Dugdale et al. 1995; Dugdale and Wilkerson 1998) envisions that diatom productivity becomes Si-limited because of the more efficient recycling of particulate organic nitrogen (PON) over biogenic silica (bSiO₂) in the euphotic zone. Zooplankton grazing on diatoms efficiently regenerates nitrogenous nutrients within the upper mixed layer but exports silica by packaging it into fecal pellets that sink to depth (Tande and Slagstad 1985; Cowie and Hedges 1996). Dissolution of bSiO₂ in the euphotic zone reduces the efficiency of the silica pump by recycling bSiO₂ back to the dissolved silicon pool before it can be exported. Field studies from a variety of oceanic sys-

tems reveal that bSiO₂ dissolution in the upper mixed layer is substantial and sustains a significant fraction of global bSiO₂ production (Brzezinski and Nelson 1989; Nelson et al. 1995; Nelson and Dortch 1996). Expressed as an integrated dissolution:production rate ratio ($\int D:\int P$), the fraction of bSiO₂ production supported by regenerated Si in the surface ocean is highly variable ($\int D:\int P = 0.05\text{--}5.8$; Nelson et al. 1995), although on mean, D:P is quite high. Nelson et al. (1995) estimated that the global mean $\int D:\int P$ is 0.6 in the upper 200 m (i.e., 60% of global diatom production is supported by recently dissolved silica frustules).

In view of the importance of bSiO₂ dissolution in the ocean silica cycle, it is critical to elucidate the mechanisms that mediate and regulate it. Seawater is undersaturated with respect to bSiO₂, so that any silica surface that is directly exposed to seawater will undergo chemical dissolution. Diatom frustules are protected from dissolution by the organic fraction of the cell wall that prevents direct contact between the silica frustule and seawater. Several biotic and abiotic factors are known to affect the rate of silica dissolution, including temperature (Kamatani 1982; Bidle et al. 2002), the surface area of silica exposed to seawater (Hurd and Birdwhistell 1983), grazing (Tande and Slagstad 1985; Jacobson and Anderson 1986), and diatom aggregation (Nelson et al. 1995; Brzezinski et al. 1997a). We recently found that bacterial ectoprotease action on marine diatom detritus strongly accelerates silica dissolution rates by removing the organic coating that protects frustules from direct exposure to seawater (Bidle and Azam 1999). This mechanism could enhance bSiO₂ dissolution rates in the euphotic zone, creating a leak in the silica pump and retaining Si in surface waters. Furthermore, species-specific variability in the effectiveness of bacteria in removing the organic matrix enveloping diatom frustules might contribute to the variability in $\int D:\int P$ ratios observed in the sea (Bidle and Azam 2001).

Here, we field test the hypothesis that proteolytic removal of the organic matrix protecting diatom frustules by specific bacterial phylotypes significantly accelerates bSiO₂ dissolution rates in situ and contributes to the variability in $\int D:\int P$ ratios in the sea. We chose the Monterey, California, upwelling system as our study site because diatoms have been shown to dominate primary productivity in these waters, as inferred from Si(OH)₄ control of new production (White and Dugdale 1997). Furthermore, Brzezinski et al. (1997b) found that this area experienced very high bSiO₂ production rates during upwelling; in fact, their measured rates were the highest ever recorded in the world ocean. These high rates were deemed to be the result of an inefficient silica pump, since an average of 72% of the bSiO₂ produced during this study remained in the surface waters and resulted in very high concentrations of biogenic silica (6.7–13.7 $\mu\text{mol Si L}^{-1}$). The high diatom biomass in this system facilitates measurement of dissolution rates enabling us to measure both bSiO₂ production and dissolution and to determine how bacteria affect the dissolution to production rate ratio.

Methods

Study site and sampling—Sampling was conducted aboard the R/V *Point Sur*, 10–21 April 2000, in the Monterey, Cal-

ifornia, upwelling system. A rosette system equipped with 10-liter Niskin bottles fitted with silicone springs and a seabird CTD was used to collect samples from an upwelling zone near Monterey Bay, California. Sampling was in two modes following Brzezinski et al. (1997b). First, a grid of 20 stations was surveyed (10–12 April) to characterize water types in the upwelling system (*see* fig. 1 in Brzezinski et al. 2003). A suite of parameters (temperature; salinity; concentrations of silicic acid, bSiO₂ and lithogenic silica; bSiO₂ production) was measured for seawater collected at 5 m depth (light depth to $\sim 54\%$ surface irradiance, I₀). Extensive measurements of bSiO₂ cycling and bacterial activity were subsequently performed at 10 profile stations (Stas. 1, 3–11), located both inside the upwelling plume and in the relatively oligotrophic waters offshore (*see* fig. 1 in Brzezinski et al. [2003] for station locations). At each profile station, water was sampled at 6 depths corresponding to 100, 54, 16, 3.6, 0.6, and 0.1% I₀. Profiles extended from the surface to between 20 and 80 m, depending on water clarity. The entire contents of each Niskin bottle was drained into a 10-liter polypropylene carboy shielded with black plastic and mixed to homogenize the particles. All samples were drawn from the 10-liter carboys. Samples were incubated on deck in a clear acrylic incubator with plastic neutral density screens and window screening to simulate in situ light intensities (0.1–100% I₀) and flowing surface seawater to maintain temperature.

Silica cycle parameters—For most stations, silicic acid (Si(OH)₄) and bSiO₂ concentrations, as well as bSiO₂ production and dissolution rates, were measured at depths corresponding to 100, 54, 16, 3.6, 0.6, and 0.1% I₀. At Stas. 5 and 6, dissolution measurements were performed at 100, 54, and 0.6% I₀ light depths. bSiO₂ production (using ³²Si incorporation) and dissolution (using ²⁹Si isotope dilution) measurements were performed after a 24-h incubation period within deck incubators cooled with flowing surface seawater. Readers are referred to Brzezinski et al. (2003) for detailed methods and analysis of silica cycling during this study.

Inhibition and stimulation of bacterial activity—Bacterial mediation of in situ bSiO₂ dissolution was measured at the 54% I₀ light level for several stations (Stas. 3, 4, 6, 9–11) by comparing the dissolution rate in untreated control samples and in samples experiencing inhibition of bacterial activity. Measurements were also performed at 0.6% I₀ for Stas. 9–11. A cocktail consisting of antibiotics (100 $\mu\text{g ml}^{-1}$ benzyl penicillin and 50 $\mu\text{g ml}^{-1}$ chloramphenicol) and protease inhibitors (170 $\mu\text{g ml}^{-1}$ phenylmethylsulfonyl fluoride, PMSF, and 0.5 $\mu\text{g ml}^{-1}$ leupeptin) was added to water samples to inhibit bacterial activity during 24-h incubations.

We also tested whether increased bacterial activity resulted in elevated bSiO₂ dissolution. Water samples at Stas. 4 and 6 were augmented with bacterial assemblages that had previously been exposed to freshly made diatom detritus. Fresh diatom detritus was produced by collecting natural diatom assemblages from Monterey Bay water onto 47-mm, 3- μm pore size polycarbonate filters and subjecting them to seven freeze-thaw cycles. Natural bacterial assemblages devoid of higher trophic levels (e.g., protozoa) were obtained

from 0.6- μm pore size filtrates under 5 cm Hg vacuum (Bidle and Azam 1999). Diatom detritus was added to natural bacterial assemblages at six times the in situ diatom cell concentration and incubated for 24 h in the dark at surface water temperature. At the end of the 24-h incubation period, each enrichment was shaken vigorously to dislodge loosely attached bacteria and was filtered under heavy vacuum with a 3- μm pore size polycarbonate filter to remove diatoms and other large particulate material. Total seawater samples were inoculated with the filtrate containing the stimulated microbial community at one-tenth the final incubation volume. Total bacterial abundance in augmented samples increased by less than a factor of two.

Bacterial abundance and activity—The abundance and metabolic activity of attached marine bacteria were measured (at the time of collection and after 24 h incubation) for each profile station at depths corresponding to 100, 54, and 0.6% I_0 , except for Sta. 11, where all six profile depths were examined. Abundance and activity of attached bacteria in inhibited and augmented samples were compared to untreated controls. Detailed methodology has been described (Bidle and Azam 1999, 2001). Bacterial abundance, enzymatic activity, and production were measured in the total and <3.0- μm filtered samples. Values for attached bacteria represent the differences between the total and <3.0- μm fractions.

Following preservation of total seawater with 2% formalin, bacterial abundance was determined by epifluorescence microscopy using diamidino-2-phenylindole (DAPI; Porter and Feig 1980). Samples were processed within a few hours of collection. Ectohydrolytic enzyme activities (protease, glucosidase, lipase, and phosphatase) were determined at each profile station using commercially available substrates containing either amino-4-methylcoumarin (AMC) or methylumbelliferone (MUF) as a fluorophore (Hoppe 1983). Fluorogenic analog substrates (Leuine-AMC, MUF- α -D-glucoside, MUF- β -D-glucoside, MUF-oleate, MUF-phosphate) were added at 20 $\mu\text{mol L}^{-1}$ final concentration. Depth-integrated enzyme activities of attached bacteria ($\mu\text{mol m}^{-2} \text{h}^{-1}$) were calculated from trapezoidal integration of activities measured at individual depths ($\text{nmol L}^{-1} \text{h}^{-1}$). Bacterial production was measured by ^3H -leucine (Kirchman et al. 1985) and ^3H -thymidine incorporation (Fuhrman and Azam 1982) using the centrifugation method (Smith and Azam 1992). Substrates were added to samples at 20 nmol L^{-1} final concentration and incubated for 0.37–2.15 h depending on biomass and expected growth rates. Assays were done in triplicate with a trichloroacetic acid-treated sample serving as a control. Cell-specific growth rate calculations for bacteria assumed 20 fg C cell $^{-1}$ (Lee and Fuhrman 1987).

Identity of bacterial colonizers—The identity of colonizing bacteria was determined by denaturing gradient gel electrophoresis (DGGE; Muyzer et al. 1993) and sequencing of 16S rDNA genes (see Bidle and Azam 2001 for details). Briefly, ~300 ml of total water samples were gravity filtered onto 47 mm of 3- μm pore size PCTE membrane filters. Filters were placed in a sterile centrifuge tube and immediately frozen (-20°C) until later processing in the laboratory. DNA

from material collected onto 3- μm pore size filters was extracted according to Fuhrman et al. (1988) with volume modification (described in Bidle and Azam 2001). 16S rDNA genes were PCR amplified using a bacteria-specific (341F) primer and a universal (534R) primer with a 40 bp GC clamp to prevent complete melting of amplicons during DGGE (Sheffield et al. 1989; Muyzer et al. 1993). Amplicons were subjected to DGGE (8% acrylamide and 30–50% denaturing gradients) to separate bands of unique phylotypes. They were excised, cloned, and sequenced. Sequences were aligned to known sequences using BLAST (Basic Local Alignment Search Tool; Altschul et al. 1990). Phylogenetic relationships were inferred by the neighbor-joining method using CLUSTAL W (Thompson et al. 1994).

^{32}Si -labeled diatom detritus— ^{32}Si -labeled diatom detritus was created to investigate the ability of natural bacterial assemblages in Monterey Bay to facilitate dissolution of diatom silica of a constant quality. Batch cultures of axenic *Thalassiosira weissflogii* (CCMP1051) and *Chaetoceros simplex* (CCMP199) were grown in 10-ml f/2 liquid medium (Guillard 1975) supplemented with 1.33×10^7 Bq ^{32}Si (specific activity = 39,000 Bq [$\mu\text{g Si}$] $^{-1}$) by rotary shaking (70 rpm) under a 14:10 light:dark cycle. Illumination was provided by cool white light fluorescent bulbs at a photon fluence rate of ~200 mol quanta $\text{cm}^{-2} \text{s}^{-1}$. The $^{32}\text{Si}(\text{OH})_4$ stock solution was cleaned of trace metals by passage through Chelex resin prior to use (Brzezinski and Phillips 1997). Cultures were harvested at ~ 10^5 cells ml^{-1} by centrifugation (3,000 \times g; 10 min), washed free of unincorporated ^{32}Si with several changes of 0.2- μm filtered, autoclaved seawater (FASW) and resuspended in FASW. Liquid scintillation counting (LSC) revealed that cells contained 5.3 Bq ^{32}Si cell $^{-1}$. Cell suspensions were made into diatom detritus by cycling the cells between rapid freezing (dry ice/ethanol bath) and thawing (55°C water bath) seven times. Lack of cellular ATP or growth in f/2 medium confirmed in a previous test of the procedure that cells were dead. CHN analysis of detritus indicated that 70–90% of total C and N was POM (unpubl. data) and suggested that the organic matrix was intact. Detritus was stored at $<-20^\circ\text{C}$ until further use.

Ability of bacterial assemblages to facilitate bSiO_2 dissolution— ^{32}Si -labeled *T. weissflogii* and *C. simplex* detritus was added to replicate seawater samples (54% I_0 , Stas. 1, 3–8; 0.6% I_0 , Sta. 1 only) at a final $\text{b}^{32}\text{SiO}_2$ concentration of 0.84 $\mu\text{mol Si L}^{-1}$ (~200 cells ml^{-1}). $\text{b}^{32}\text{SiO}_2$ dissolution was determined by measuring the ^{32}Si released into solution over the course of 17–19 d. Samples were removed every day for the first week; subsequent samples were removed every few days. Detritus additions corresponded to 9–20% of the existing bSiO_2 pool for all stations except Sta. 6, where detritus additions increased the bSiO_2 pool sixfold because of low existing bSiO_2 concentration (0.14 $\mu\text{mol Si L}^{-1}$). Abiotic controls consisted of ^{32}Si -labeled detritus incubating in 0.2- μm filtered, autoclaved seawater. Incubations were performed in the dark at sea surface temperature in acid-washed (10% HCl), sterile, 125-ml polycarbonate erlenmeyer flasks. In order to guard against the uptake of dissolving ^{32}Si by living diatoms in the natural population and a potential re-

duction in our ^{32}Si dissolution signal, samples were incubated in the dark for at least 12 h prior to addition of ^{32}Si -labeled detritus. Silicon uptake requires a source of energy so cells stop taking it up after ~ 24 h in the dark (Blank and Sullivan 1979). Also, the ambient silicon concentration was increased several-fold by adding sterile NaSiO_3 to each flask at a final concentration of $50 \mu\text{mol Si L}^{-1}$; potential uptake of ^{32}Si would be reduced by the same proportion. Ambient silicon concentrations were $0.34\text{--}4.66 \mu\text{mol Si L}^{-1}$ at 54% I_0 for these stations prior to NaSiO_3 addition. Aliquots (~ 10 ml) were removed from samples and centrifuged ($3,000 \times g$; 10 min) to pellet diatom cells. Three milliliters of the supernatant was removed for LSC (in duplicate) to determine the amount of ^{32}Si that had entered solution from the labeled silica detritus. Care was taken so that, after processing, at least 4 ml of supernatant volume remained above the pellet, minimizing the risk of contamination of ^{32}Si from the pellet. Samples were counted using 10 ml of LSC cocktail (Optima Gold, Packard Instrument) as described by Brzezinski and Phillips (1997).

Results

Characteristics of the study site—Physical and chemical properties at the survey stations revealed the presence of upwelled water (cold, high salinity) centered on the north end of Monterey Bay (see fig. 2 in Brzezinski et al. 2003). Elevated concentrations of bSiO_2 indicated a moderate diatom bloom. Diatom assemblages were dominated by *Skeletonema* spp. but also consisted of *Chaetoceros* spp. and *Thalassiosira* spp. Profile stations were located both within and outside the upwelling plume (see figs. 1 and 2 in Brzezinski et al. 2003) and exhibited a variety of silicon dynamics (see table 1 in Brzezinski et al. 2003). Integrated bSiO_2 concentration ($\int [\text{bSiO}_2]$) between the surface and the 0.1% light depth ranged from 16.3 to 175 mmol Si m^{-2} among profile stations, with 7 of 10 stations exhibiting concentrations $>100 \text{mmol Si m}^{-2}$. A large range was also observed in integrated silica production rates ($\int \rho_b$) with values from 4.8 to 108 $\text{mmol Si m}^{-2} \text{d}^{-1}$ among profile stations. Six of eight stations had $\int \rho_b > 29 \text{mmol Si m}^{-2} \text{d}^{-1}$. In general, stations with elevated $\int [\text{bSiO}_2]$ and $\int \rho_b$ were near the upwelling plume or within Monterey Bay. These stations had a mean $\int \text{D} : \int \text{P}$ of 0.06 ± 0.03 . Depth profiles of two characteristic “high-biomass” stations revealed minimal depth variation in the specific bSiO_2 dissolution rate (V_{dis}) and D:P ratio (Fig. 1).

Stations 6 and 9 had very different silicon dynamics with $\int [\text{bSiO}_2] < 45 \text{mmol Si m}^{-2}$ and $\int \rho_b < 6 \text{mmol Si m}^{-2} \text{d}^{-1}$ (see table 1 in Brzezinski et al. 2003). Although the total amount of silica dissolving in the euphotic zone ($\int \rho_{\text{dis}}$) was comparable to other stations, Stas. 6 and 9 were characterized by both higher average V_{dis} and $\int \text{D} : \int \text{P}$. These stations also displayed considerable increases in V_{dis} and D:P ratio with depth (Fig. 1).

There was some concern that incubation of deeper samples with warmer surface seawater artificially elevated dissolution rates, especially at low-biomass stations, since the 0.6% I_0 light depth extended deeper in the water column (70

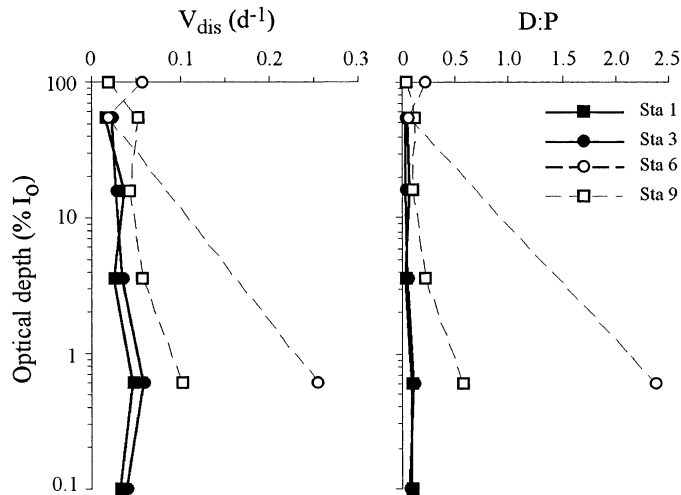


Fig. 1. Depth profiles of the specific silica dissolution rate (V_{dis}) and the silica dissolution:production rate ratio (D:P) at stations characterized by high (Stas. 1 and 3) and low (Stas. 6 and 9) siliceous biomass. D:P ratios were determined from absolute silica production (ρ_b) and silica dissolution (ρ_{dis}) rates. Problems with sample recovery prevented accurate dissolution measurement at 0.1% I_0 for Sta. 9.

and 80 m). The surface water used to maintain the temperature of on-deck incubations was $0\text{--}2.9^\circ\text{C}$ warmer than water at the 0.6% I_0 light depth (Table 1). We had previously shown that temperature significantly regulated bacteria mediation of silica dissolution (Bidle et al. 2002). Using pooled data for bSiO_2 dissolution of *T. weissflogii*, *S. costatum*, and natural diatom assemblages incubating at various temperatures (Kamatani 1982; Bidle et al. 2002), we determined an empirical relationship between V_{dis} and temperature (Fig. 2) and calculated the degree to which incubation with warmer surface seawater artificially elevated dissolution rates of 0.6% I_0 water samples. Small differences in V_{dis} ($0.001\text{--}0.004 \text{d}^{-1}$) were calculated for diatom assemblages incubating at either the in situ 0.6% I_0 temperature or surface seawater temperature (ΔV_{dis} in Table 1). Thus, only $0\text{--}4.7\%$ of the measured V_{dis} for 0.6% I_0 light depths could be attributed to elevated incubation temperature. The respective contribution at Stas. 6 and 9 was 1.7 and 1.8%. A similar analysis for water collected at the 54% I_0 light depth showed that $0\text{--}2.8\%$ of the observed V_{dis} could be accounted for by incubation at surface water temperature. The temperature difference between these two depths was $0\text{--}0.4^\circ\text{C}$ over all stations.

Effectiveness of inhibition and augmentation—After sampling Sta. 1, we discovered that the PMSF in the full inhibitor cocktail, although effective at inhibiting bacterial activity, was problematic. Its addition caused an unexpected, unidentified precipitate to form in the seawater, decreased bSiO_2 production by $>95\%$, and interfered with silicic acid recovery for bSiO_2 dissolution measurements. For this reason, dissolution data are not reported for full cocktail treatment. We altered the inhibitor cocktail for all subsequent stations to consist of leupeptin, penicillin, and chloramphenicol. This cocktail inhibited bacterial activity but did not in-

Table 1. The difference in seawater temperature (ΔT) at profile stations between 100% and 0.6% I_0 light depths and its calculated contribution to observed V_{dis} at the 0.6% I_0 light depth.

Station	Temperature ($^{\circ}\text{C}$)			V_{dis} (d^{-1})		
	100% I_0	0.6% I_0	ΔT	0.6% I_0^*	$\Delta\dagger$	%
1	10.9	10.3	0.6	0.047	0.001	1.7
3	11.3	10.2	1.1	0.058	0.002	2.6
4	12.1	10.2	1.9	—	—	—
5	11.5	10.0	1.5	0.055	0.002	3.7
6	12.9	10.0	2.9	0.255	0.004	1.7
7	11.5	11.5	0.0	0.045	0.000	0.0
8	12.5	11.4	1.1	—	—	—
9	12.3	11.1	1.2	0.101	0.002	1.8
10	12.9	12.5	0.4	—	—	—
11	12.7	12.2	0.5	0.017	0.001	4.7

* In situ V_{dis} .

† The difference in calculated V_{dis} between the 100% and 0.6% I_0 water temperatures; calculated from relationship presented in Fig. 2.

terfere with dissolution measurements. This treatment did reduce bSiO_2 production by 60–70%.

V_{dis} was reduced at all but one station when bacterial activity was inhibited (Table 2, upper portion). The mean reduction in V_{dis} was $44 \pm 27\%$ ($n = 6$) over 24 h. The degree of inhibition varied from 22 to 91% among stations at the 54% I_0 light depth, with the largest effect (65–91%) being observed at low-biomass Stas. 6 and 9. High-biomass stations were characterized by 22–33% reduction in V_{dis} . Inhibition at the 0.6% I_0 light depth reduced V_{dis} by 22% at Sta. 9. Problems in sample recovery prevented accurate measurements of dissolution at 0.6% I_0 for Sta. 10. Of natural diatom assemblages receiving treatment, Sta. 11 was the only one that displayed either no change or an increase in V_{dis} . The inhibitor cocktail was effective at reducing dissolution of ^{32}Si -labeled detritus at Stas. 7 and 8 but not Sta. 6,

where it led to a 22–23% increase in V_{dis} (Table 2, lower portion). However, it is worth noting that the V_{dis} for untreated samples at Sta. 6 was similar to, but 12 and 44% greater than, abiotic controls. Control-corrected V_{dis} values at this station went from 0.001 to 0.003 d^{-1} for *T. weissflogii* and from 0.004 to 0.007 d^{-1} for *C. simplex* after inhibitor treatment. Augmenting natural samples with a stimulated bacterial community (Stas. 4 and 6) had no effect on V_{dis} .

Exposure to the inhibitor cocktail for 24 h diminished the abundance, cell-specific ectoproteolytic activity, and production of attached bacteria by 44–63%, 54–88%, and >99%, respectively, compared to controls. Ranges include data for all stations tested (Sta. 3, 4, 6, 10) at both the 54 and 0.6% light levels. The inhibitor cocktail minimally inhibited other classes of ectohydrolytic enzymes; cell-specific glucosidase and lipase activities were either unchanged or increased slightly (by $<5 \text{ amol cell}^{-1} \text{ h}^{-1}$). In augmented samples, bacterial abundance, protease activity, and production increased by as much as 489, 245, and 513%, respectively, after 24 h.

We calculated the effect of inhibition or augmentation on the removal of diatom particulate organic carbon (POC) in Monterey Bay samples on the basis of data from previous laboratory experiments (Bidle et al. 2002). In these lab-based experiments, proteolytic hydrolysis ($\mu\text{mol substrate hydrolyzed L}^{-1} \text{ h}^{-1}$) and POC regeneration (mg C L^{-1}) were simultaneously measured over a 72-h time course for uniformly ^{14}C -labeled *T. weissflogii* detritus ($0.1295 \text{ Bq } ^{14}\text{C cell}^{-1}$; $700 \mu\text{g C L}^{-1}$ POC) incubated with natural bacterial assemblages at 15°C . The hydrolysis rates measured at individual time points were time-integrated, in order to obtain the cumulative proteolytic hydrolysis exerted on detritus over the incubation time ($\mu\text{mol substrate hydrolyzed L}^{-1}$), and empirically related to diatom POC regeneration (Fig. 3). Regeneration of diatom POC in Monterey Bay samples was calculated by applying measured proteolytic hydrolysis (24-h incubation period) to this relationship. On the basis of this analysis, the regeneration of diatom POC in untreated control samples was calculated at $0.06\text{--}0.21 \text{ mg C L}^{-1} \text{ d}^{-1}$. Exposure to the inhibitor cocktail led to 40–76% reductions in calculated POC regeneration, whereas samples augmented

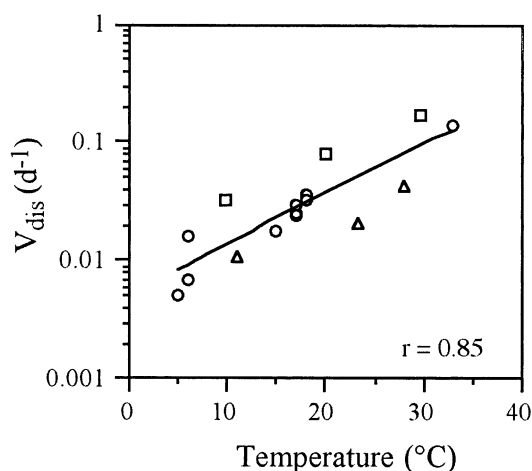


Fig. 2. Dependence of V_{dis} on temperature. Data from two different studies were pooled. They include *T. weissflogii* detritus (circles) incubating in surface seawater containing natural bacterial assemblages (Bidle et al. 2002), *S. costatum* cells (squares), and natural diatom assemblages (triangles) incubating in $0.45\text{-}\mu\text{m}$ filtered, near-surface seawater (Kamatani 1982). Line represents an exponential regression ($y = 0.005 \times 10^{0.042x}$).

Table 2. The effect of bacterial inhibition on the specific dissolution rate of diatom silica. Results for two different sample types are presented. The upper portion of the table refers to 24-h incubations containing both in situ bacterial and diatom assemblages. The lower portion of the table corresponds to 17–19-d incubations containing in situ bacterial assemblages and ^{32}Si -labeled, axenic diatom detritus.

Source of bSiO_2	Station	% I_0	V_{dis} (d^{-1})		% reduction*
			Control	Inhibited	
Natural diatom assemblages					
	3	54	0.025	0.019	24
	4	54	0.010	0.007	30
	6	54	0.011	0.001	91
	9	54	0.052	0.018	65
		0.6	0.101	0.079	22
	10	54	0.015	0.010	33
		0.6	—	—	—
	11	54	0.023	0.023	0
		0.6	0.017	0.022	(29)
Detritus					
<i>T. weissflogii</i>	6	54	0.009	0.011	(22)
	7	54	0.029	0.007	76
	8	54	0.024	0.006	75
	Control†	—	0.008	—	—
<i>C. simplex</i>	6	54	0.013	0.016	(23)
	7	54	0.036	0.014	61
	8	54	0.044	0.035	20
	Control†	—	0.009	—	—

* Parentheses designate an increase in V_{dis} .

† Detritus incubating in filtered, autoclaved seawater.

with a stimulated bacterial community displayed a 14–33% increase.

Relationship between bacteria and silicon parameters.— Abundance ($r = 0.84$, $p < 0.001$), cell-specific protease activity ($r = 0.86$, $p < 0.001$), and bacterial production ($r = 0.66$, $p < 0.005$) of attached bacteria were significantly correlated with $[\text{bSiO}_2]$ (Fig. 4). Analysis included data from every station and sampling depth for which these corresponding parameters were measured. Data adhered to assumptions for parametric analysis.

We examined whether proteolytic hydrolysis and production of attached bacteria were correlated with two different silica dissolution parameters in the euphotic zone (Fig. 5). $\int \rho_{\text{dis}}$ represents dissolution occurring throughout the euphotic zone, whereas V_{dis} represents the relative dissolution at individual depths (V_{dis} is the dissolution rate, ρ_{dis} , normalized to bSiO_2 biomass). Data for high- and low-biomass stations are plotted separately. Weak, insignificant ($r < 0.44$; $p > 0.32$) relationships were observed between both depth-specific bacterial activity measurements and corresponding bSiO_2 dissolution parameters.

We also integrated protease activity to a given depth and compared that to bSiO_2 dissolution with the argument that dissolution was due to bacterial action on diatoms sinking from the surface to that depth. We reasoned that proteolytic enzymes will likely remain active on sinking diatoms even after bacterial physiology is compromised. Integrated protease activities were strongly correlated ($r > 0.91$, $p < 0.001$) with $\int \rho_{\text{dis}}$ regardless of biomass load (Fig. 6A).

Strong correlation was also observed between integrated protease activity and the V_{dis} measured at the deepest point of integration for stations characterized by low ($r = 0.95$, $p < 0.005$) and high ($r = 0.79$, $p < 0.001$) diatom biomass (Fig. 6B). The former displayed much higher V_{dis} at much lower integrated protease activities.

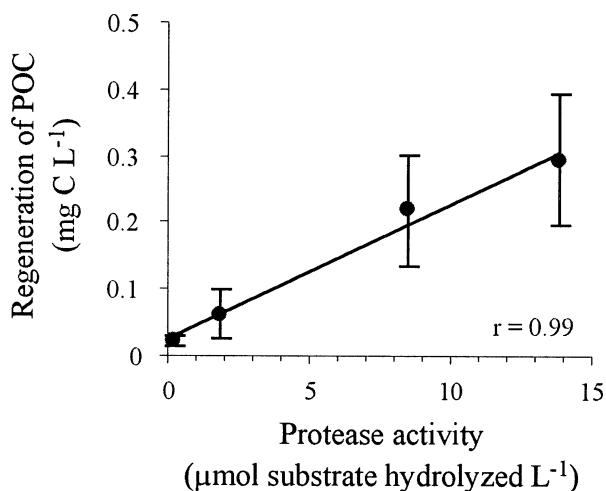


Fig. 3. Dependence of POC regeneration from *T. weissflogii* detritus on proteolytic hydrolysis by attached bacteria over a 72-h incubation period (POC regeneration = $0.0203 \times$ protease activity + 0.0276). Error bars represent the standard deviation among triplicate samples. Correlation coefficient (r) for linear regression is given.

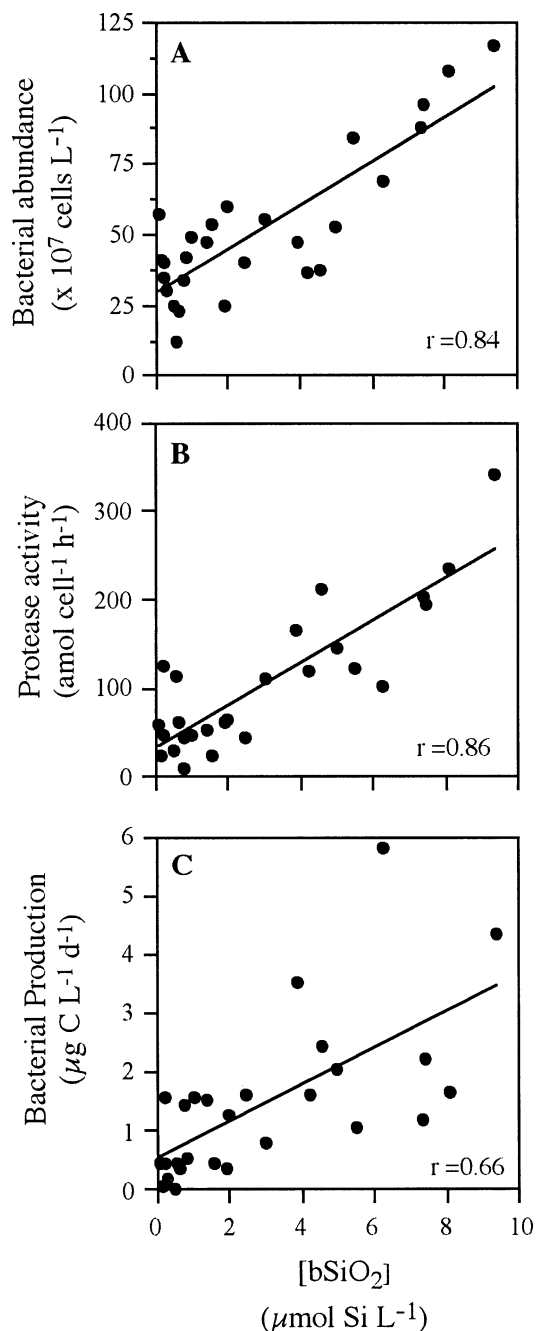


Fig. 4. Relationship between (A) abundance, (B) cell-specific protease activity, and (C) bacterial production of in situ attached bacterial assemblages and diatom biomass (expressed as biogenic silica concentration). Data are presented for samples from all profile stations. Correlation coefficients (r) for linear regression are provided in each panel.

Ability of bacterial communities to facilitate silica regeneration—The potential of natural bacterial assemblages to facilitate bSiO_2 dissolution from ^{32}Si -labeled *T. weissflogii* and *C. simplex* detritus varied threefold among different stations at 54% I_0 (Fig. 7, upper panel). V_{dis} was 0.009–0.032 d^{-1} for *T. weissflogii* and 0.013–0.044 d^{-1} for *C. simplex*. Much of this variability was due to the ineffectiveness of

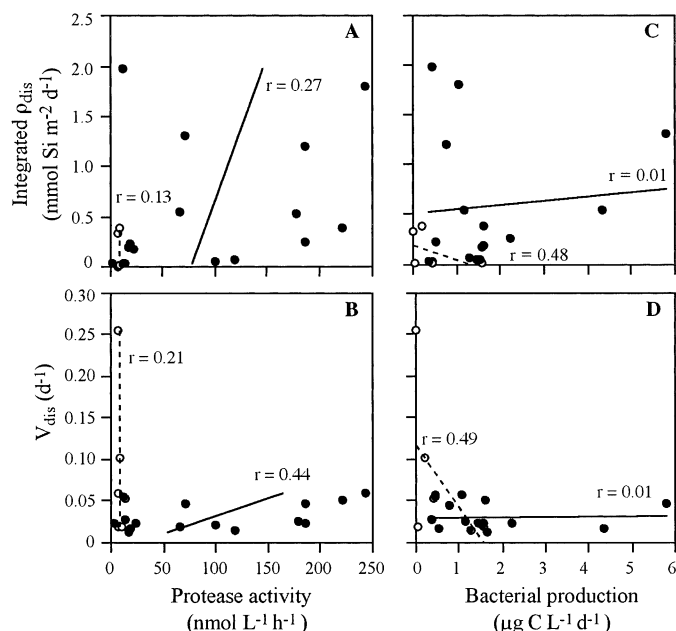


Fig. 5. Relationship between depth-specific activity of attached bacterial assemblages and silica dissolution of diatom assemblages. Values were measured at a particular sampling time and depth. (A–B) Protease activity based on the hydrolysis rate of Leu-AMC. (C–D) Bacterial production based on the uptake of leucine. Diatom silica dissolution is presented both as the depth-integrated silica dissolution rate ($\int \rho_{\text{dis}}$) and the specific biogenic silica dissolution rate (V_{dis}) at a particular depth. The latter is normalized to bSiO_2 concentration. $\int \rho_{\text{dis}}$ was calculated from dissolution rate measurements over a complete depth profile. Correlation coefficients are given in each panel. Open circles/dashed line, Stas. 6 and 9 (low bSiO_2); filled circles/solid line, Stas. 1, 3, 5, 7, 10, and 11 (high bSiO_2).

bacterial assemblages at Sta. 6 to facilitate bSiO_2 dissolution from either labeled diatom. V_{dis} was only 12 and 44% higher than abiotic seawater incubations (Table 2, lower portion; compared to 250–388% increases in V_{dis} for bacterial assemblages collected from Stas. 7 and 8). In contrast, high-biomass stations displayed consistently high V_{dis} ($>0.020 \text{ d}^{-1}$). The abundance, proteolytic activity, and production for bacterial assemblages from Sta. 6 were $4.1 \times 10^8 \text{ cells L}^{-1}$, $51.2 \text{ amol cell}^{-1} \text{ h}^{-1}$, and $0.04 \mu\text{g C L}^{-1} \text{ d}^{-1}$, respectively. The same parameters, averaged among high-biomass stations, were $5.7 (\pm 3.5) \times 10^8 \text{ cells L}^{-1}$, $155.1 (\pm 68.8) \text{ amol cell}^{-1} \text{ h}^{-1}$, and $2.5 (\pm 1.2) \mu\text{g C L}^{-1} \text{ d}^{-1}$, respectively.

Natural assemblages collected from two different depths at Sta. 1 displayed similar ability to facilitate bSiO_2 dissolution (Fig. 7, lower panel).

Taxonomy of colonizing bacteria—DGGE profiles of bacterial communities in the $>3.0 \mu\text{m}$ size fraction provided a fingerprint of bacterial colonization dynamics and bacterial species richness (i.e., number of bands). The DGGE profile shown for Sta. 4 (Fig. 8) was representative of the general colonization dynamics for untreated and treated samples. The predominance of particular bacterial phylotypes in this size fraction suggested that they played a role in silica dis-

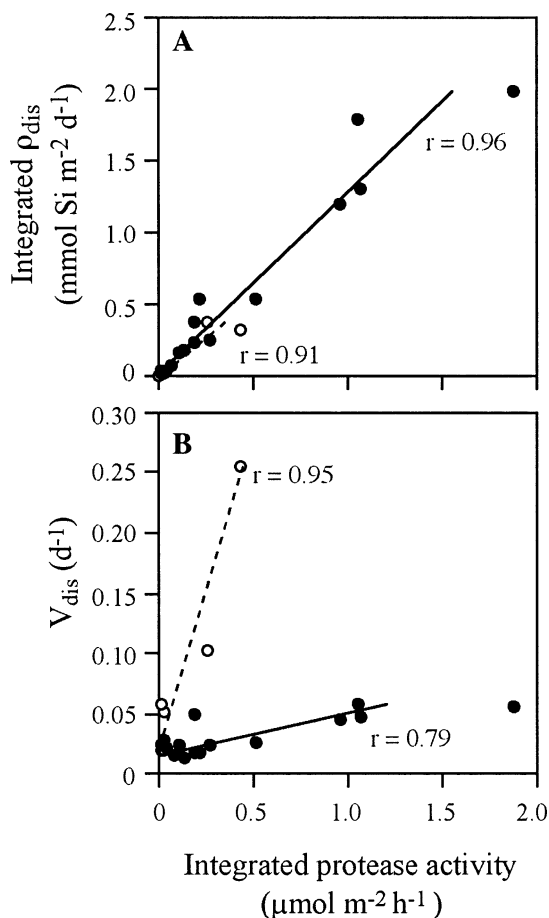


Fig. 6. Relationship between depth-integrated, proteolytic hydrolysis and silica dissolution parameters (A) $\int \rho_{\text{dis}}$ and (B) V_{dis} . Integrated proteolytic hydrolysis was calculated from measurements of activity at three different depths (corresponding to 100, 54, and 0.6% I_0 light levels), except for Sta. 11, where a complete depth profile was done. Symbols are the same as in Fig. 5.

solution by colonizing and degrading diatom organic matter. Even though DGGE analysis of PCR amplicons has potential biases, it reflects the major variations in the relative abundance of PCR-amplifiable phylotypes. Replicate PCR and DGGE gels confirmed that profiles are highly reproducible, leading us to assume there is a comparable amplification bias for or against a certain sequence (Bidle and Azam 2001). Thus, we assumed that changes in the relative band intensity with time reflect actual changes in the relative abundance of a phylotype. We recognize that DGGE does not provide a complete or quantitative view of bacterial community composition, but rather a more simplified "fingerprint."

Inhibitor cocktails had different effects on the community composition of attached bacteria after 24 h of exposure. Full inhibitor treatment (including PMSF) significantly altered the community composition. Three unique bacterial phylotypes (MODE-6, -15, and -18) appeared, whereas MODE-14, a diatom-related phylotype, disappeared. Inhibition with leupeptin, penicillin, and chloramphenicol had relatively little effect, with the only notable change being reduced band intensity for MODE-14. DGGE profiles for augmented sam-

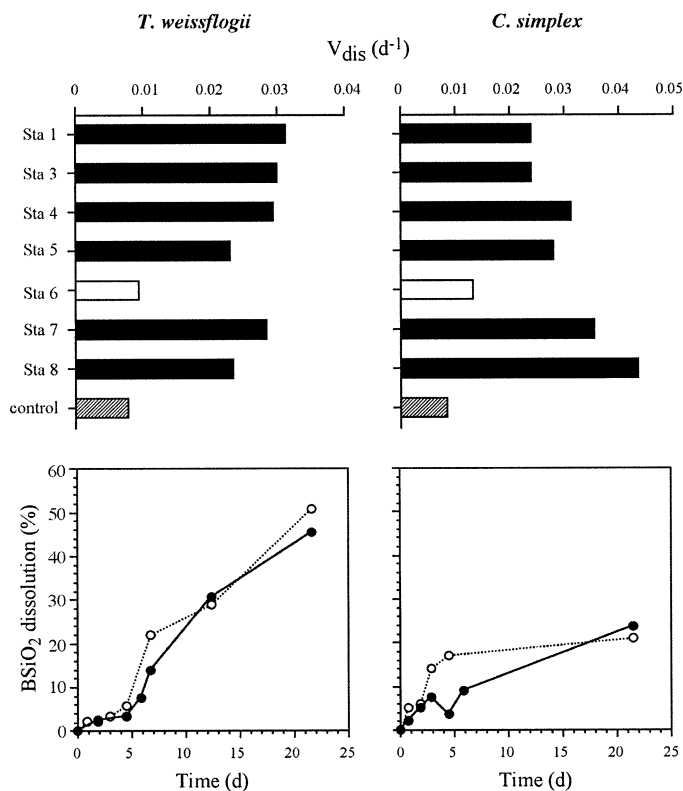


Fig. 7. Ability of in situ natural bacterial assemblages from different stations to regenerate silicic acid from ^{32}Si -labeled *T. weissflogii* (*T.w.*) and *C. simplex* (*C.s.*) detritus. (Upper panel) V_{dis} of ^{32}Si -labeled diatom detritus after 17–19 d. Low-biomass Sta. 6 is indicated by open bar. Control incubation (hatched bar) represents detritus incubating in abiotic seawater. Data is for natural bacterial assemblages collected from the 54% I_0 light level. (Lower panel) Time course of Si regeneration for natural assemblages collected at different depths at Sta. 1 (closed symbols = 54% I_0 , 4 m; open symbols = 0.6% I_0 , 20 m). Data corresponds to the V_{dis} reported in the upper panel (*T.w.*, $0.032 \pm 0.003 \text{ d}^{-1}$; *C.s.*, $0.023 \pm 0.001 \text{ d}^{-1}$).

ples, including the enriched, 0.6- μm filtrate used as an inoculum, mirrored those seen for untreated controls, indicating that our enrichment procedure did not significantly alter the dominant community composition of colonizing phylotypes.

We surveyed the dominant phylotypes associated with the $>3.0\text{-}\mu\text{m}$ community at all profile stations by sequencing unique bands in DGGE profiles (Table 3). Many phylotypes were closely related to plastid 16S rRNA genes from a variety of eukaryotic phytoplankton (Fig. 9). Nearly 60% of these phylotypes were closely related to plastid genes of diatoms (note their close relationship to *T. weissflogii* 16S rRNA). The remaining plastid phylotypes represented haptophyte and prasinophyte groups. Representatives from the Cytophaga/Flavobacteria/Bacteriodes (CFB) were detected among the $>3.0\text{-}\mu\text{m}$ community at all profile stations. They comprised 44% of the unique, bacterial phylotypes excised and sequenced from DGGE analysis. Members of the α , β , γ , and ϵ subclasses of *Proteobacteria* were also associated with bloom particles with α - and γ -*Proteobacteria* being detected at all profile stations. γ -*Proteobacteria* accounted for

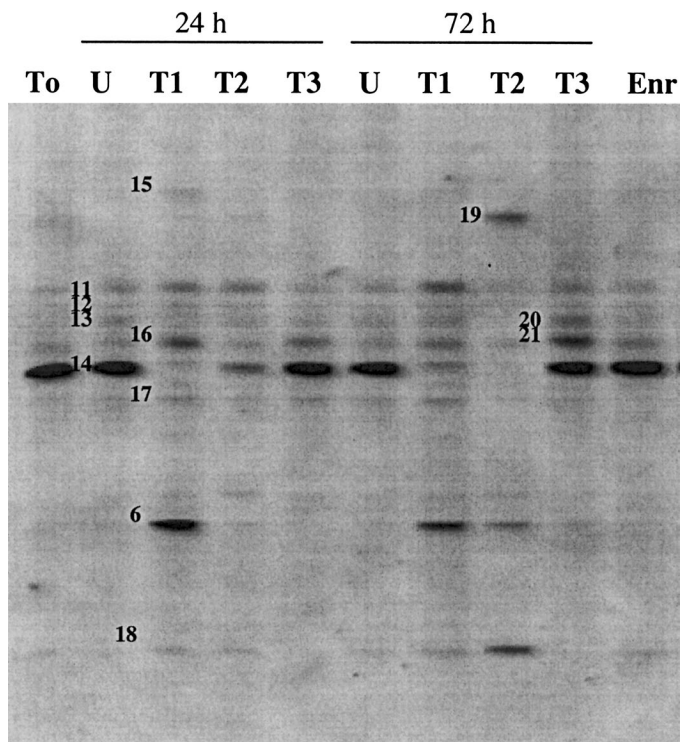


Fig. 8. DGGE profiles characterizing the community composition of bacteria associated with the $>3.0\text{-}\mu\text{m}$ size fraction at the 54% light depth (6 m) from Sta. 4. Denaturing gradient was 30–55%. Results are shown for the original seawater sample (T_0) as well as for 24- and 72-h treatment incubations (Un, untreated; T1, inhibitor treatment with PMSF; T2, inhibitor treatment without PMSF; T3, bacterial stimulation treatment; Enr, bacterial enrichment used to inoculate T3). Each excised, cloned, and sequenced band is numbered. The relationships of excised band sequences to other sequences in the GenBank database are listed in Table 3 (“MODE” prefix is added to band number).

24% of sequenced bacterial phylotypes, with many being closely related to bacterial phylotypes causing enhanced Si regeneration (Bidle and Azam 2001). We detected a eukaryotic phylotype (MODE-11) most closely related to 18S rDNA from the copepod *Cancerincola plumipes* at a majority of stations.

Discussion

We encountered a diatom bloom within upwelled water centered on the north side of Monterey Bay consisting primarily of *Skeletonema costatum*, but also containing *Chaetoceros* spp. and *Thalassiosira* spp. The mean $\int [\text{bSiO}_2]$ ($116 \text{ mmol Si m}^{-2}$) and $\int \rho_b$ ($55 \text{ mmol Si m}^{-2} \text{ d}^{-1}$) at 7 of the 10 stations were similar to those reported for the Baja California, northwest Africa, and Peru upwelling systems (mean = $49.4 \text{ mmol m}^{-2} \text{ d}^{-1}$ for 69 profiles; Nelson et al. 1995) but were lower than those previously reported for Monterey Bay ($205 \text{ mmol Si m}^{-2} \text{ d}^{-1}$; Brzezinski et al. 1997b). Stations 6 and 9 were characterized by dramatically lower mean $\int [\text{bSiO}_2]$ ($19 \text{ mmol Si m}^{-2}$) and $\int \rho_b$ ($5 \text{ mmol Si m}^{-2} \text{ d}^{-1}$), making them similar to reports from a Gulf Stream warm-

core ring (Brzezinski and Nelson 1989) and the Sargasso Sea (Brzezinski and Nelson 1995). These conditions provided a unique opportunity to assess bacterial regulation of bSiO_2 dissolution rates under high and low silicon and diatom concentrations.

A significant correlation between $[\text{bSiO}_2]$ and abundance, cell-specific protease activity, and production of attached bacteria suggested that bacterial colonization and subsequent physiological activity were coupled to diatom biomass. A direct role for bacteria in facilitating bSiO_2 dissolution within the euphotic zone was experimentally tested using treatments designed to inhibit the activity of bacteria. A variety of selective metabolic inhibitors of bacterioplankton and protozoa, including antibiotics, have successfully been used to determine the role of the microbial loop in marine food webs (Sherr et al. 1986; Oremland and Capone 1988). Our strategy also used a protease inhibitor (leupeptin) because protease action by bacteria was found to regulate bSiO_2 dissolution in laboratory experiments (Bidle and Azam 1999, 2001) and because proteolytic enzymes can remain active even after bacterial physiology becomes compromised (Smith et al. 1992). The effectiveness of the inhibitor treatment of field samples was verified in incubations using intact ^{32}Si -labeled *T. weissflogii* and *C. simplex* detritus that had not previously experienced enzymatic degradation. Inhibitor treatment reduced V_{dis} by 20–76% for high-biomass stations. A reduction in V_{dis} was not observed for Sta. 6, probably because bacterial assemblages were relatively unable to facilitate bSiO_2 dissolution. In untreated samples, they exhibited very low V_{dis} values corrected for abiotic controls. This inability was apparently due to the very low level of proteolytic activity and production of attached bacteria at Sta. 6 compared to high-biomass stations, rather than lower abundance of attached bacteria. Respective cell-specific protease activity and bacterial production of attached bacteria were 3- and 62-fold lower at Sta. 6 than at high-biomass stations, whereas bacterial abundance was similar.

A 24-h treatment with inhibitor cocktail reduced the V_{dis} of field samples by an average of $44 \pm 27\%$ ($n = 6$, range 22–91%), illustrating that the activity of colonizing bacteria is a variable regulator of bSiO_2 dissolution within the euphotic zone. A similar degree of inhibition was observed for the abundance, protease activity, and production of attached bacteria, confirming that observed reductions in bSiO_2 dissolution were due to inhibition of bacterial activity. A reduction in protease activities implied a reduction in the removal of organic matter protecting diatom frustules from dissolution. Using an empirical relationship from previous lab studies (Bidle et al. 2002; Fig. 3), we translated the proteolytic hydrolysis exerted on diatoms over the course of an experiment into the amount of diatom POC released. We then calculated the effect that reduced proteolytic hydrolysis would have on the removal of protective organic matter in Monterey samples. That analysis indicated that POC regeneration in untreated control samples ($0.06\text{--}0.21 \text{ mg C L}^{-1} \text{ d}^{-1}$) was reduced by 40–76% in the presence of inhibitors. A similar analysis allowed us to assess why the samples augmented with stimulated bacteria were less effective at increasing dissolution rates, even though attached bacterial protease activity increased by 245%. Measured proteolytic

Table 3. Relationship of excised band sequences to other sequences in the GenBank database. Underlining designates phylotypes (or closest relatives to phylotypes) that were previously documented colonizers facilitating regeneration of diatom silica (Bidle and Azam 2001).

Clone ID	Accession number*	Closest relative† (% identity)	Phylogenetic grouping	Stations detected
MODE-1	AF419351	Marine bacterium MBIC1357 (98)	CFB	1,3,7,8
MODE-2	AF419352	Marine bacterium MBIC1357 (98)	CFB	1,3
MODE-3	AF419353	Uncultured marine eubacterium MBE6 (82)	Chloroplast	1,3,7,8
MODE-4	AF419354	Uncultured marine <i>Cytophaga</i> MBE2	CFB	1,3
MODE-5	AF419355	<i>Pseudomonas pickettii</i> ‡ (93/289)	<i>γ-Proteobacteria</i>	1,3
MODE-6	AF419356	Uncultured marine bacterium COL-22‡ (100)	<i>γ-Proteobacteria</i>	1,3–6,9–11
MODE-7	AF419357	<i>Comamonas acidovorans</i> MC1‡ (100)	<i>β-Proteobacteria</i>	1,3
MODE-8	AF419358	Marine psychrophile SW17 (95)	CFB	1,3,7–11
MODE-9	AF419359	<i>Comamonas acidovorans</i> MC1‡ (99)	<i>β-Proteobacteria</i>	1,3
MODE-10	AF419360	Uncultured <i>Roseobacter</i> NAC1–4‡ (99)	<i>α-Proteobacteria</i>	1,3
MODE-11	AF419361	<i>Cancrincola plumipes</i> (98)	Eukaryota; copepod	1,3–5,7–11
MODE-12	AF419362	Uncultured phytoplankton ESR 1‡ (100)	chloroplast	3–11
MODE-13	AF419363	Marine bacterium MBIC1357 (96)	CFB	3,4
MODE-14	AF419364	<i>Amphora delicatissima</i> (97)	Phytoplankton	3,4
MODE-15	AF419365	Cytophagales strain MED10 (93)	CFB	3–6
MODE-16	AF419366	Marine bacterium MBIC1357 (96)	CFB	3,4
MODE-17	AF419367	Uncultured marine eubacterium HstpL29 (98)	Cyanobacteria	3,4
MODE-18	AF419368	<i>Afipia felis</i> ‡ (100)	<i>α-Proteobacteria</i>	3,4
MODE-19	AF419369	<i>Pseudomonas</i> sp. FSL R1–195‡ (100)	<i>γ-Proteobacteria</i>	4
MODE-20	AF419370	Uncultured Crater Lake bacterium CL 120–102 (97)	chloroplast	3,4
MODE-21	AF419371	Uncultured marine eubacterium OTU_C (99)	CFB	3,4
MODE-22	AF419372	<i>Bradyrhizobium</i> sp. strain Cj3–3‡ (100)	<i>α-Proteobacteria</i>	3,4,6,9–11
MODE-23	AF419373	Uncultured marine <i>Cytophaga</i> MBE2 (100)	CFB	6
MODE-24	AF419374	Environmental clone OCS20‡ (100)	chloroplast	6
MODE-25	AF419375	Unidentified eukaryote clone OM20 (97)	Plastid	6
MODE-26	AF419376	Uncultured marine bacterium COL-13 (100)	<i>γ-Proteobacteria</i>	6
MODE-27	AF419377	<i>Amphora delicatissima</i> (99)	chloroplast	6
MODE-28	AF419378	Uncultured phytoplankton ESR 1‡ (99)	plastid	6
MODE-29	AF419379	Environmental clone OCS182 (100)	chloroplast	6
MODE-30	AF419380	<i>Pseudoalteromonas</i> sp. AP-28‡ (99)	<i>γ-Proteobacteria</i>	6
MODE-31	AF419381	Marine bacterium Tw-7‡ (100)	<i>γ-Proteobacteria</i>	5–8
MODE-32	AF419382	Uncultured Crater Lake bacterium CL0–117 (89)	<i>α-Proteobacteria</i>	6
MODE-33	AF419383	Uncultured <i>ε-Proteobacterium</i> VC1.2-cl18‡ (95)	<i>ε-Proteobacteria</i>	6
MODE-34	AF419384	Uncultured marine bacterium ZD0255 (98)	CFB	6
MODE-35	AF419385	Uncultured phytoplankton ESR 1‡ (99)	plastid	5
MODE-36	AF419386	Uncultured marine eubacterium MBE6 (100)	plastid	5,7,8
MODE-37	AF419387	Uncultured marine eubacterium MBE6 (98)	plastid	5,7,8
MODE-38	AF419388	Unidentified eukaryote clone (OM20 (97)	plastid	5,7,8
MODE-39	AF419389	Uncultured marine bacterium COL-35 (93)	CFB	9–11
MODE-40	AF419390	Uncultured prasinophyte clone OM39 (100)	chlorophyta	9–11
MODE-41	AF419391	Uncultured marine eubacterium MBE6 (98)	plastid	9–11
MODE-42	FA419392	<i>Comamonas acidovorans</i> MC1‡ (99)	<i>β-Proteobacteria</i>	1–3

* For sequences obtained in this study; nucleotide sequences can be accessed at <http://www.ncbi.nlm.nih.gov/>.

† Sequences were aligned to the closest relative using BLAST (Altschul et al. 1990). Identities were calculated excluding gaps.

‡ Clone sequence had multiple relatives with same percent identity.

hydrolysis in augmented samples corresponded to a 14–33% increase in POC regeneration and, hence, only modestly increased the amount of bSiO₂ exposed for dissolution. The observation that V_{dis} at Sta. 11 did not change or increase in the presence of inhibitors suggested that bacterial assemblages did not influence bSiO₂ dissolution at this location. This was puzzling given that the abundance, proteolytic activity, production, and dominant phylotypes of attached bacteria were similar to other profile stations, where reductions in V_{dis} were observed (e.g., Stas. 9 and 10). It is possible that addition of inhibitors to this sample led to physiological

effects that increased bSiO₂ dissolution rates (discussed below).

Several lines of evidence suggested that our field results underestimated bacterially mediated bSiO₂ dissolution. First, inhibition treatments reduced protease activity of attached bacteria but did not completely abolish it. Residual activity likely contributed to dissolution during incubations. Second, with the exception of Sta. 6 where V_{dis} was similar to abiotic controls, inhibitor treatment was effective for incubations with intact, ³²Si-labeled diatom detritus (i.e., not experiencing prior degradation). Unfortunately, diatom history cannot

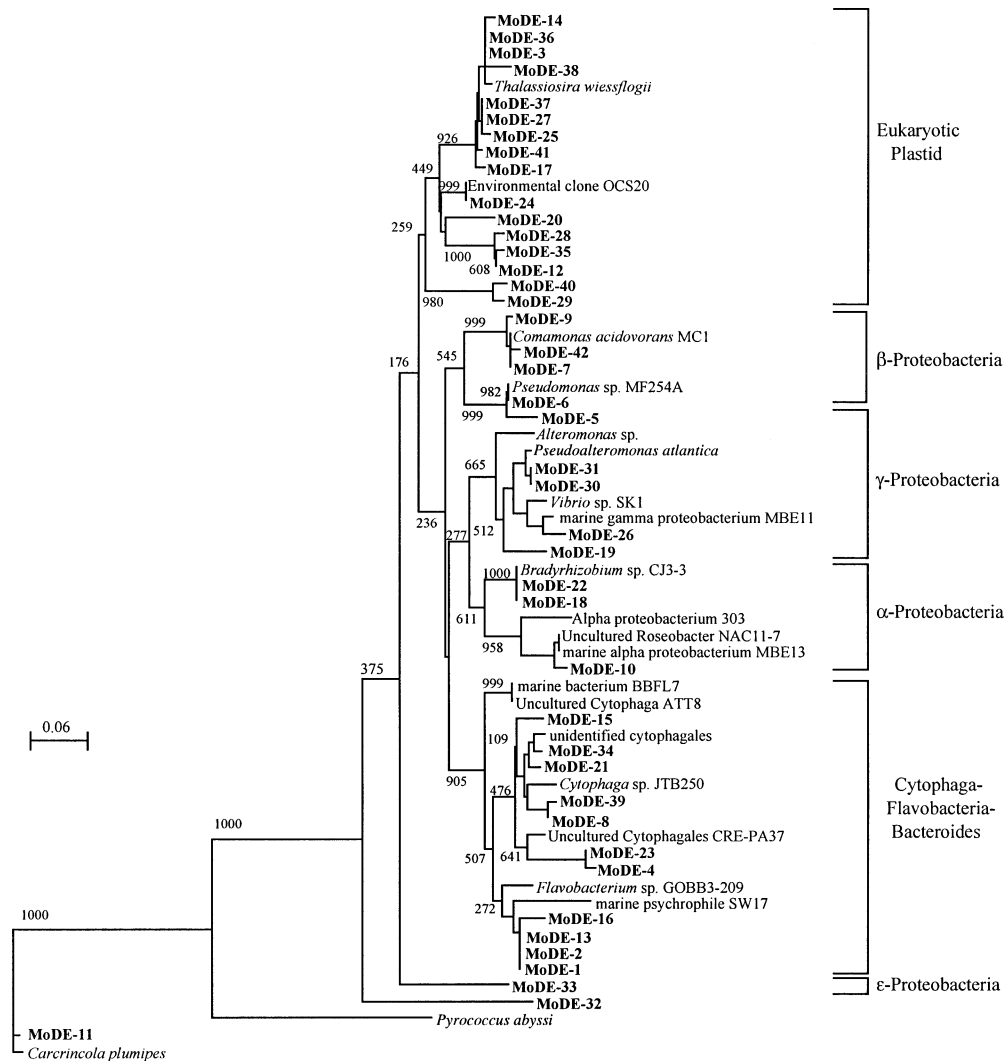


Fig. 9. Phylogenetic tree illustrating the relationships of sequenced bands (bold type) to major classes of bacteria and phytoplankton. The tree was inferred by the neighbor-joining method (CLUSTAL W; Thompson et al. 1994) using the entire length of sequenced bands (~ 194 bp) beginning at the equivalent base to 341 and going toward the 3' end of the 16S rRNA gene (*Escherichia coli* numbering). An archaeon, *Pyrococcus abyssi* ST549, was used as an outgroup. The number of bootstrap replicates supporting the branching order is shown above relevant nodes (out of 1,000 replicate samples). Scale bar indicates base pair substitutions per nucleotide position.

be controlled during natural blooms. Proteolytic degradation of the natural diatom assemblages that had occurred prior to sampling would have been unaffected by inhibition treatments and likely contributed to bSiO_2 dissolution during our incubations. Third, inhibitor treatment clearly stressed cells by inhibiting bSiO_2 production. Diatoms respond to physiological stress by lysing (Berges and Falkowski 1998), e-fluxing internal pools of dissolved silicon (Martin-Jézéquel et al. 2000), or both. Inhibitor treatment likely led to both an increase in the proportion of detrital cells vulnerable to bacterial attack and the release of internal Si pools into the surrounding seawater. The ^{29}Si isotope dilution technique cannot distinguish between Si that enters solution via dissolution and that which enters solution because of the release of intracellular Si pools, so both processes might have in-

creased V_{dis} in inhibitor treatments. In studies with natural diatom assemblages, we observed decreases in V_{dis} at all but one station, illustrating that the effect of inhibiting bacterial activity on lowering dissolution rates overwhelmed any physiological effects that would artificially increase dissolution rates.

Exposure of in situ bacterial communities from different stations (54% I_0) to axenic, ^{32}Si -labeled, diatom detritus was used as a proxy for their inherent potential to facilitate bSiO_2 dissolution. Dissolution was measured over a longer time scale (17–19 d incubation) in these incubations compared to unamended water samples (24-h incubation) because of the use of diatoms that had not experienced prior degradation. Nonetheless, V_{dis} for incubations with ^{32}Si prelabeled diatoms ($0.009\text{--}0.044\text{ d}^{-1}$) generally agreed very well with in

situ V_{dis} values (0.011–0.052 d^{-1}) at most stations. This was not the case for Sta. 6, however. Bacterial assemblages at this location displayed low V_{dis} values against intact laboratory-made diatom detritus (Table 2, lower section; Fig. 7, upper panel) but comparable (and often greater) in situ V_{dis} than those determined for the high-biomass stations (Fig. 1). Molecular analysis of the bacterial phylotypes associated with resident diatom assemblages revealed no striking difference in composition between low- and high-biomass stations, even though low-biomass stations were less effective against intact diatom detritus. Similar dominant phylotypes were detected at all stations, with many being very closely related to effective “recyclers” of diatom silica (Bidle and Azam 2001). Low activity of attached bacteria at Sta. 6, rather than differences in abundance and community composition, was responsible for the inherently low facilitation of bSiO_2 dissolution from diatom detritus. Elevated in situ V_{dis} values observed at this station, however, were likely due to unique characteristics of resident diatom assemblages (discussed below).

We anticipated that the role of bacteria in mediating bSiO_2 dissolution might increase with depth because V_{dis} is often lowest in the upper few meters of the water column and increases significantly in the lower euphotic zone (Nelson and Goering 1977; Nelson and Gordon 1982; Brzezinski and Nelson 1989). Our results suggest that increases in V_{dis} with depth are not caused by the presence of more active bacterial assemblages deeper in the euphotic zone. Correlation between both proteolytic hydrolysis and bacterial production of attached bacteria at a given depth to bSiO_2 dissolution rates at those depths was weak and insignificant (Fig. 5). Also, we found bacterial communities collected from the 54 and 0.6% light levels at Sta. 1 facilitated bSiO_2 dissolution equally well ($V_{\text{dis}} = 0.032\text{--}0.036 \text{ d}^{-1}$ for *T. weissflogii*; $0.022\text{--}0.024$ for *C. simplex*). Instead, integrated protease activities, accounting for the cumulative effect of proteolytic attack over the depth range sampled, strongly correlated with dissolution rates measured at the depth of the lower bound of the integration. Indeed, laboratory microcosm experiments have demonstrated that significant POC removal (>30%) from diatom detritus is required before appreciable bSiO_2 dissolution is realized (Bidle et al. 2002). Therefore, higher V_{dis} at depth reflects the cumulative effect of bacterial colonization and degradation of particles containing diatoms as the particles sink through the water column.

The physiological state and history of resident diatoms likely influenced bacterial mediation of bSiO_2 dissolution. During blooms, diatom populations go through varied physiological and nutritional states relevant to issues of bacteria–diatom interactions. As a consequence, bSiO_2 dissolution (and the contribution of resident bacterial colonizers) likely varies as a bloom develops and finally enters senescence, when it is more susceptible to bacterial attack. At Stas. 6 and 9, relatively low protease activities ($0.007\text{--}0.430 \mu\text{mol m}^{-2} \text{ h}^{-1}$) caused extensive in situ V_{dis} but minimal V_{dis} from ^{32}Si -labeled detritus. Our findings are consistent with the probability that diatom assemblages at Stas. 6 and 9 were at the terminus of the bloom and Si-limited, leading to a high fraction of detrital silica, compromised silica frustules, or both. Stations 6 and 9 had silicic acid concentrations

($[\text{Si}(\text{OH})_4]$) of $<6 \mu\text{mol Si L}^{-1}$ and $<5 \mu\text{mol Si L}^{-1}$, respectively, down to the 3.6% I_0 light depth (30 and 25 m). They were also characterized by low $[\text{bSiO}_2]$ throughout the euphotic zone. The $[\text{bSiO}_2]$ was $<0.8 \mu\text{mol Si L}^{-1}$ and $<0.3 \mu\text{mol Si L}^{-1}$, respectively, down to the 0.1% I_0 light depth (80 and 70 m). Previous kinetic studies of diatom communities in the Monterey upwelling system have revealed a K_s for silicic acid uptake at $4.2 \mu\text{mol Si L}^{-1}$ (White and Dugdale 1997) and limitation of bSiO_2 production at $5 \mu\text{mol Si L}^{-1} \text{ Si}(\text{OH})_4$ (Brzezinski et al. 1997b). During our cruise, silica limitation was detected at Sta. 5 (only station tested); V_b increased three- to sixfold when the ambient $[\text{Si}(\text{OH})_4]$ ($0.70\text{--}1.40 \mu\text{mol Si L}^{-1}$) was increased to $30 \mu\text{mol Si}(\text{OH})_4 \text{ L}^{-1}$ (Brzezinski unpubl. data). Si-limited diatoms can display reduced silicification (i.e., thinner frustules) (Paasche 1975; Davis 1976; Harrison et al. 1977; Brzezinski et al. 1990) and exhibit more extensive dissolution than those with thick frustules at similar protease activities (Bidle and Azam 1999).

The balance between integrated bSiO_2 dissolution and integrated bSiO_2 production ($\int \text{D} : \int \text{P}$) in the euphotic zone is a key determinant of the strength of the silica pump. Bloom events have a high potential for accelerating the silica pump with $\int \text{D} : \int \text{P} < 0.10$ (Brzezinski et al. 2003). In this Monterey study, the mean $\int \text{D} : \int \text{P}$ at high-biomass bloom stations was 0.06 ± 0.03 . Silica pump strength is likely significantly weakened during nonbloom periods since a majority of silica production is recycled within the euphotic zone. $\int \text{D} : \int \text{P}$ ratios of 0.6–0.8 have been reported for the oligotrophic ocean (Brzezinski and Nelson 1995; Nelson and Brzezinski 1997). In our study, Stas. 6 and 9 exhibited oligotrophic bSiO_2 characteristics and displayed $\int \text{D} : \int \text{P}$ of 0.61 and 0.13, respectively. High V_{dis} at the 0.6% light level at Stas. 6 (0.255 d^{-1}) and 9 (0.101 d^{-1}) contributed to dramatic increases in the D:P ratio, with Sta. 6 experiencing net dissolution ($\text{D} : \text{P} > 2.5$). Extensive silicon regeneration exhibited in nonbloom systems (e.g., oligotrophic gyres) (Brzezinski and Nelson 1989, 1995) could be widespread in the sea and might not require high proteolytic hydrolysis by the microbial loop because of the presence of fragile diatoms. Indeed, an $\int \text{D} : \int \text{P}$ in excess of 0.50 is required for nonbloom systems in order to reconcile very low $\int \text{D} : \int \text{P}$ (<0.10) for blooms and the global mean $\int \text{D} : \int \text{P}$ of 0.5–0.6 (Brzezinski et al. 2003).

This study is the first to directly document bacterial mediation of bSiO_2 dissolution among natural diatom communities and provide mechanistic insight to explain increasing V_{dis} with depth within the upper 80 m in field studies. We were able to directly measure bacterial mediation of bSiO_2 dissolution in a high-export, coastal upwelling system, where $\int \text{D} : \int \text{P}$ was <0.10 , and demonstrate that the microbial loop causes a leak in the silica pump by accelerating the rate of silicic acid regeneration in the euphotic zone. At this study site, silica was being regenerated at a rate that was only slightly slower than that for PON (Brzezinski et al. 2003), confirming earlier estimates that, although the silica pump applies to the Monterey upwelling system, it is fairly weak (Brzezinski et al. 1997b). By recycling particulate silica back into the dissolved silicon reservoir, bacteria diminish the efficiency at which silica is exported and lower the potential for Si limitation in the euphotic zone. Because this process involves the degradation of organic matter, the export of di-

atom POC and PON is simultaneously diminished. Bacterial regulation of silica pump efficiency will depend on factors that couple diatom biomass to the microbial loop, such as zooplankton grazing. Macrozooplankton grazing in the euphotic zone would have a predicted negative influence on coupling to the microbial loop because of the production of rapidly sinking fecal pellets. Alternatively, grazing could serve to “prepare” living diatoms for subsequent colonization and proteolytic attack by making them into detritus (Tande and Slagstad 1985; Cowie and Hedges 1996). Fragments of diatom frustules released during fecal pellet degradation have negligible sinking rates and might have represented significant Si regeneration within the upper 40–110 m of a warm-core ring (Bishop et al. 1986; Brzezinski and Nelson 1989). Our results confirm predictions from lab-based experiments that colonization of diatom frustules and proteolytic attack by bacterial colonizers facilitates bSiO₂ dissolution in the sea. The consistency of mechanistic controls between lab and field studies underscores their importance in the oceanic silica cycle and suggests that they should be incorporated into biogeochemical models.

References

- ALTSCHUL, S. F., W. GISH, W. MILLER, E. W. MYERS, AND D. J. LIPMAN. 1990. Basic local alignment search tool. *J. Mol. Biol.* **215**: 403–410.
- BERGES, J. A., AND P. G. FALKOWSKI. 1998. Physiological stress and cell death in marine phytoplankton: Induction of proteases in response to nitrogen or light limitation. *Limnol. Oceanogr.* **43**: 129–135.
- BIDLE, K. D., AND F. AZAM. 1999. Accelerated dissolution of diatom silica by natural marine bacterial assemblages. *Nature* **397**: 508–512.
- , AND ———. 2001. Bacterial control of silicon regeneration from diatom detritus: Significance of bacterial ectohydrolases and species identity. *Limnol. Oceanogr.* **46**: 1606–1623.
- , M. MANGANELLI, AND F. AZAM. 2002. Regulation of oceanic silicon and carbon preservation by temperature control on bacterial activity. *Science* **298**: 1980–1984.
- BISHOP, J. M., M. CONTE, P. H. WIEBE, M. R. ROMAN, AND C. LANGDON. 1986. Particulate matter production and consumption in deep mixed layers: Observations in a warm-core ring. *Deep-Sea Res.* **33**: 1813–1841.
- BLANK, G. S., AND C. W. SULLIVAN. 1979. Diatom mineralization of silicic acid III. Si(OH)₄ binding and light dependent transport in *Nitzschia angularis*. *Arch. Microbiol.* **123**: 157–163.
- BRZEZINSKI, M. A., AND D. M. NELSON. 1989. Seasonal changes in the silicon cycle within a Gulf Stream warm-core ring. *Deep-Sea Res.* **36**: 1009–1030.
- , AND ———. 1995. The annual silica cycle in the Sargasso Sea near Bermuda. *Deep-Sea Res. I* **42**: 1215–1237.
- , AND ———. 1996. Chronic substrate limitation of silicic acid uptake rates in the western Sargasso Sea. *Deep-Sea Res. II Top. Stud. Oceanogr.* **43**: 437–453.
- , AND D. R. PHILLIPS. 1997. Evaluation of ³²Si as a tracer for measuring silica production rates in marine waters. *Limnol. Oceanogr.* **42**: 856–865.
- , R. J. OLSEN, AND S. W. CHISHOLM. 1990. Silicon availability and cell-cycle progression in marine diatoms. *Mar. Ecol. Prog. Ser.* **67**: 83–96.
- , A. L. ALLDREDGE, AND L. M. O'BRYAN. 1997a. Silica cycling within marine snow. *Limnol. Oceanogr.* **42**: 1706–1713.
- , D. R. PHILLIPS, F. P. CHAVEZ, G. E. FRIEDERICH, AND R. C. DUGDALE. 1997b. Silica production in the Monterey, California, upwelling system. *Limnol. Oceanogr.* **42**: 1694–1705.
- , T. A. VILLAREAL, AND F. LIPSCHULTZ. 1998. Silica production and the contribution of diatoms to new and primary production in the central North Pacific. *Mar. Ecol. Prog. Ser.* **167**: 89–104.
- , J. JONES, K. BIDLE, AND F. AZAM. 2003. The balance between silica production and silica dissolution in the sea. Insights from Monterey Bay, California, applied to the global data set. *Limnol. Oceanogr.* **48**: 1846–1854.
- COWIE, G. L., AND J. I. HEDGES. 1996. Digestion and alteration of the biochemical constituents of a diatom (*Thalassiosira weissflogii*) ingested by a herbivorous zooplankton (*Calanus pacificus*). *Limnol. Oceanogr.* **41**: 581–594.
- DAVIS, C. O. 1976. Continuous culture of marine diatoms under silicate limitation. II. Effect of light intensity on growth and nutrient uptake of *Skeletonema costatum*. *J. Phycol.* **12**: 291–300.
- DUGDALE, R. C., AND F. P. WILKERSON. 1998. Silicate regulation of new production in the equatorial Pacific upwelling. *Nature* **391**: 270–273.
- , ———, AND H. J. MINAS. 1995. The role of a silicate pump in driving new production. *Deep-Sea Res. I* **42**: 697–719.
- FUHRMAN, J. A., AND F. AZAM. 1982. Thymidine incorporation as a measure of heterotrophic bacterioplankton production in marine surface waters: Evaluation and field results. *Mar. Biol.* **66**: 109–120.
- , D. E. COMEAU, Å. HAGSTROM, AND A. M. CHAN. 1988. Extraction from natural planktonic microorganisms of DNA suitable for molecular biological studies. *Appl. Environ. Microbiol.* **54**: 1426–1429.
- GUILLARD, R. R. L. 1975. Culture of phytoplankton for feeding marine invertebrates, pp. 26–60. *In* W. L. Smith and M. H. Chanley [ed.], *Culture of marine invertebrate animals*. Plenum.
- HARRISON, P. J., H. L. CONWAY, R. W. HOLMES, AND C. O. DAVIS. 1977. Marine diatoms grown in chemostats under silicate or ammonium limitation. III. Cellular composition and morphology of *Chaetoceros debilis*, *Skeletonema costatum*, and *Thalassiosira gravida*. *Mar. Biol.* **43**: 19–31.
- HOPPE, H. G. 1983. Significance of exoenzymatic activities in the ecology of brackish water: Measurements by means of methylumbelliferyl-substrates. *Mar. Ecol. Prog. Ser.* **11**: 299–308.
- HURD, D. C., AND S. BIRDWHISTELL. 1983. On producing a general model for biogenic silica dissolution. *Am. J. Sci.* **283**: 1–28.
- JACOBSON, D. M., AND D. M. ANDERSON. 1986. Thecate heterotrophic dinoflagellates: Feeding behavior and mechanisms. *J. Phycol.* **22**: 249–258.
- KAMATANI, A. 1982. Dissolution rates of silica from diatoms decomposing at various temperatures. *Mar. Biol.* **68**: 91–98.
- KIRCHMAN, D., E. K'NEES, AND R. HODSON. 1985. Leucine incorporation and its potential as a measure of protein synthesis by bacteria in natural aquatic systems. *Appl. Environ. Microbiol.* **49**: 599–607.
- LEE, S., AND J. A. FUHRMAN. 1987. Relationships between biovolume and biomass of naturally derived marine bacterioplankton. *Appl. Environ. Microbiol.* **53**: 1298–1303.
- LEWIN, J. C. 1962. Silicification, pp. 445–455. *In* R. E. Lewin [ed.], *Physiology and biochemistry of algae*. Academic.
- MARTIN-JÉZÉQUEL, V., M. HILDEBRAND, AND M. A. BRZEZINSKI. 2000. Silicon metabolism in diatoms: Implications for growth. *J. Phycol.* **36**: 821–840.
- MUYZER, G., E. C. D. WAAL, AND A. G. UITTERLINDEN. 1993. Pro-

- filing of complex microbial populations by denaturing gradient gel electrophoresis analysis of polymerase chain reaction-amplified genes coding for 16S rRNA. *Appl. Environ. Microbiol.* **59**: 695–700.
- NELSON, D. M., AND M. A. BRZEZINSKI. 1990. Kinetics of silicic acid uptake by natural diatom assemblages in two Gulf Stream warm-core rings. *Mar. Ecol. Prog. Ser.* **62**: 283–292.
- , AND ———. 1997. Diatom growth and productivity in an oligotrophic midocean gyre: A 3-yr record from the Sargasso Sea near Bermuda. *Limnol. Oceanogr.* **42**: 473–486.
- , AND Q. DORTCH. 1996. Silicic acid depletion and silicon limitation in the plume of Mississippi River: Evidence from kinetic studies in spring and summer. *Mar. Ecol. Prog. Ser.* **136**: 163–178.
- , AND J. J. GOERING. 1977. Near-surface silica dissolution in the upwelling region off northwest Africa. *Deep-Sea Res.* **24**: 65–73.
- , AND L. I. GORDON. 1982. Production and pelagic dissolution of biogenic silica in the Southern Ocean. *Geochim. Cosmochim. Acta* **46**: 491–501.
- , AND P. TRÉGUER. 1992. Role of silicon as a limiting nutrient to Antarctic diatoms: Evidence from kinetic studies in the Ross Sea ice-edge zone. *Mar. Ecol. Prog. Ser.* **80**: 255–264.
- , ———, M. A. BRZEZINSKI, A. LEYNAERT, AND B. QUÉGUINER. 1995. Production and dissolution of biogenic silica in the ocean: Revised global estimates, comparison with regional data and relationship to biogenic sedimentation. *Glob. Biogeochem. Cycles* **9**: 359–372.
- OREMLAND, R. S., AND D. G. CAPONE. 1988. Use of specific inhibitors in microbial ecological and biogeochemical studies. *Adv. Microb. Ecol.* **10**: 285–383.
- PAASCHE, E. 1975. Growth of the plankton diatom *Thalassiosira nordenskioldii* Cleve at low silicate concentrations. *J. Exp. Mar. Biol.* **18**: 173–183.
- PORTER, K. G., AND Y. S. FEIG. 1980. The use of DAPI for identifying and counting aquatic microflora. *Limnol. Oceanogr.* **25**: 943–948.
- SHEFFIELD, V. C., D. R. COX, L. S. LERMAN, AND R. M. MYERS. 1989. Attachment of a 40-base-pair G+C-rich sequence (GC-clamp) to genomic DNA fragments by the polymerase chain reaction results in improved detection of single-base changes. *Proc. Natl. Acad. Sci. USA* **86**: 232–236.
- SHERR, B. F., E. B. SHERR, T. L. ANDREW, R. D. FALLON, AND S. Y. NEWELL. 1986. Trophic interactions between heterotrophic protozoa and bacterioplankton in estuarine water analyzed with selective metabolic inhibitors. *Mar. Ecol. Prog. Ser.* **32**: 169–179.
- SMITH, D. C., AND F. AZAM. 1992. A simple, economic method for measuring bacterial protein synthesis rates in seawater using ^3H -leucine. *Mar. Microb. Food Webs* **6**: 107–114.
- , M. SIMON, A. L. ALLDREGE, AND F. AZAM. 1992. Intense hydrolytic enzyme activity on marine aggregates and implications for rapid particle dissolution. *Nature* **359**: 139–142.
- TANDE, K. S., AND D. SLAGSTAD. 1985. Assimilation efficiency in herbivorous aquatic organisms—the potential of the ratio method using ^{14}C and biogenic silica as markers. *Limnol. Oceanogr.* **30**: 1093–1099.
- THOMPSON, J. D., D. E. HIGGINS, AND T. J. GIBSON. 1994. Clustal W: Improving the sensitivity of progressive multiple sequence alignment through sequence weighting, position-specific gap penalties and weight matrix choice. *Nucleic Acids Res.* **22**: 4673–4680.
- THOMPSON, P. 1999. Response of growth and biochemical composition to variations in day length, temperature, and irradiance in the marine diatom *Thalassiosira pseudonana* (Bacillariophyceae). *J. Phycol.* **35**: 1215–1223.
- WHITE, K. K., AND R. C. DUGDALE. 1997. Silicate and nitrate uptake in the Monterey Bay upwelling system. *Cont. Shelf Res.* **17**: 455–472.

Received: 6 May 2002

Accepted: 4 April 2003

Amended: 7 May 2003